

# Inferring epistasis from genomic data by Gaussian closure

Hong-Li Zeng,<sup>1,2,\*</sup> Eugenio Mauri,<sup>3,†</sup> Vito Dichio,<sup>4,5,6,‡</sup> Simona Cocco,<sup>3,§</sup> Rémi Monasson,<sup>3</sup> and Erik Aurell<sup>6,¶</sup>

<sup>1</sup>*School of Science, and New Energy Technology Engineering Laboratory of Jiangsu Province, Nanjing University of Posts and Telecommunications, Nanjing 210023, China*

<sup>2</sup>*Nordita, Royal Institute of Technology, and Stockholm University, SE-10691 Stockholm, Sweden* \*\*

<sup>3</sup>*Laboratory of Physics of the Ecole Normale Supérieure, CNRS UMR 8023 and PSL Research, 24 rue Lhomond, 75231 Paris cedex 05, France*\*\*

<sup>4</sup>*Department of Physics, University of Trieste, Strada Costiera 11 34151, Trieste, Italy*

<sup>5</sup>*Nordita, Royal Institute of Technology, and Stockholm University, SE-10691 Stockholm, Sweden*

<sup>6</sup>*KTH – Royal Institute of Technology, AlbaNova University Center, SE-106 91 Stockholm, Sweden*

(Dated: May 24, 2022)

We consider a population evolving due to mutation, selection, genetic drift and recombination, where selection is only two-loci terms (pairwise epistatic fitness). We further consider the problem of inferring fitness in the evolutionary dynamics from one or several snapshots of the distribution of genotypes in the population. We show that this is possible using a recently developed theory that relates parameters of such a distribution to parameters of the evolutionary dynamics. This extends classical results on the Quasi-Linkage Equilibrium (QLE) regime first obtained by Kimura, and more recently studied by Neher and Shraiman. In particular, the new theory outperforms the Kimura-Neher-Shraiman theory in the interesting regime where the effects of mutations are comparable to or larger than recombination. Additionally, it can work when recombination is absent. The findings are validated through numerical simulations.

## I. INTRODUCTION

Fitness as understood in this paper is the propensity of an organism to pass on its genotype to the next generation, described by a fitness value of each genotype. A set of such values is called a fitness landscape; evolution is a process whereby nature tends towards populating the peaks in the landscape [1]. Motion in fitness landscapes describes the evolution of a population of one species in a roughly constant environment. Prime examples of this are pathogens and parasites colonizing a host evolving on a much slower time scale. The most fit pathogen is then one that is best able to exploit the opportunities and weaknesses of a typical host to grow, multiply and eventually spread to other hosts. Excluded from the concept of fitness as considered here are aspects of games of competition and cooperation in evolution [2, 3].

Sequencing of genomes of human pathogens today happen on a massive scale. In an extreme example, samples of SARS-CoV-2, the etiological agent of the disease COVID-19, have by now been sequenced more than 56,400 (accessed on 2020-06-30) times, and is being sequenced several hundreds of times daily [4–6]. This virus in the betacoronavirus family has only been known to science for about six months.

It is clear that much information about the evolutionary process must be contained in such data. In particular, if genetic variants in different positions contribute synergistically to fitness this should be reflected in the distribution over genotypes. The goal of this paper is to address the basis of such an approach, and to de-

velop tools to use it better in the future. In two recent contributions [7, 8] we have argued that a natural setting is the *Quasi-Linkage Equilibrium* (QLE) phase of Kimura [9], more recently studied by Neher and Shraiman [10, 11]. When recombination (the exchange of genomic material between individuals, or sex) is a much faster process than mutations or selection due to fitness the stationary distribution over genotypes is the Gibbs-Boltzmann distribution of an Ising or Potts model. The inverse Ising/Potts [12, 13] or Direct Coupling Analysis (DCA) [14–16] methods have been invented to infer the parameters of such distributions from samples. Quantitative properties of QLE allow to go one step further, and relate those effective couplings to the parameters of the evolutionary dynamics, which we will call the Kimura-Neher-Shraiman (KNS) theory. In [8] we showed that it is indeed possible to retrieve synergistic contributions to fitness from simulated population data by KNS theory.

In the following we will present an alternative to KNS theory built on a Gaussian closure developed by three of us [17, 18]. We will show that this new theory allows for retrieving synergistic contributions to fitness in much wider parameter ranges, using only empirical correlations, and not DCA. Moreover, contrary to KNS theory, recombination (sex) is no longer required to be a much stronger process than mutations, but could actually be set to zero. The conditions on recombination compared to variations in synergistic contributions to fitness are also much less strict in the new theory.

The paper is organized as follows. In Section II we summarize evolution driven by selection, recombination and mutations, and present the new Gaussian closure of the evolutionary equations. In Section III we summarize our model and simulation strategies, and in Sections III A and III B we compare how well we are able to infer fitness when varying mutation rate, the strength of fitness variations, and the rate of recombination. In Section IV we summarize and discuss our results. Appendices contain additional material. In Appendix A we

\* hlzeng@njupt.edu.cn

† emauri@clipper.ens.psl.eu

‡ s235818@ds.units.it

§ simona.cocco@phys.ens.fr

¶ eaurell@kth.se

\*\* These two authors contributed equally

give more details of the approach of [17, 18], as a background to the presentation in Section II. Appendix B contains parameter settings for simulations of an evolving population using the FFPopSim software [19], and in Appendix C we give details on the DCA method we have used in this work.

## II. EVOLUTIONARY DYNAMICS AND GAUSSIAN CLOSURE

The forces of evolution in classical population genetics are selection, mutations and genetic drift [20, 21]. Selection confers an advantage on individuals with certain characteristics, so that they tend to have more descendants. Mutations are random changes of the genomes. Genetic drift is the element of chance as to which individual survives, and which does not. Common to these three forces is that they all act on the single genotype level: an organism survives to the next generation, or it does not. If it does it will have a number of descendants “children”, “grand-children” etc. The distribution of individuals over genotypes can then formally be written as a gain-loss process

$$\partial_t P(\mathbf{g}, t) = \sum_{\mathbf{g}'} (k_{\mathbf{g}', \mathbf{g}} P(\mathbf{g}', t) - k_{\mathbf{g}, \mathbf{g}'} P(\mathbf{g}, t)), \quad (1)$$

where the rates  $k_{\mathbf{g}', \mathbf{g}}$  encode selection and mutation, and where genetic drift appears in the finite  $N$  effects *e.g.* in a Monte Carlo simulation. As the details of relevant equations are discussed in great detail in [11] as well as more recently in [7, 8] we not state them here, but instead summarize them in Appendix A.

Recombination (or sex) is the process by which two genotypes combine to give a third one in the next generation. It cannot be expressed in the form of Eq. (1). Instead, in general terms it looks as

$$\partial_t P(\mathbf{g}, t) = \dots + \sum_{\mathbf{g}', \mathbf{g}''} C_{\mathbf{g}, \mathbf{g}', \mathbf{g}''} P_2(\mathbf{g}', \mathbf{g}'', t), \quad (2)$$

where  $P_2$  stands for the joint probability of two genotypes  $\mathbf{g}'$  and  $\mathbf{g}''$ , and  $C_{\mathbf{g}, \mathbf{g}', \mathbf{g}''}$  is the rate at which these two produce an offspring  $\mathbf{g}$ . Equation (2) is not closed; there would be an equation for  $\partial_t P_2$  which would depend on the three-genotype distribution  $P_3$ , and so on. A standard way to close such a BBKGY-like hierarchy is to assume random mating (random collisions), *i.e.*,  $P_2(\mathbf{g}', \mathbf{g}'', t) = P(\mathbf{g}', t)P(\mathbf{g}'', t)$ . Combining (1) and (2) we hence get the evolution of a population as a non-linear differential equation analogous to a Boltzmann equation. Details are again given in Appendix A.

In (1) and (2) each genotype  $\mathbf{g}$  is seen as a sequence of positions (or loci) of length  $L$ ,  $\mathbf{g} \equiv \{s_0, s_1, \dots, s_{L-1}\}$ . The variable at each position (the allele)  $s_i$  can be in one out of  $n_i$  states. In the following discussion, we simplify by taking  $n_i = 2$  such that  $s_i$  is a binary variable. Following the conventions in the physical literature, and in particular [11], we set  $s_i = \pm 1$ .

We will from now on limit ourselves to fitness landscapes that contain linear and quadratic terms in the al-

le variables. This means that the fitness of a genotype is given by a function

$$F(\mathbf{g}) = \sum_i f_i s_i + \sum_{ij} f_{ij} s_i s_j \quad (3)$$

The linear term  $f_i$  is called an *additive contribution to fitness* while the quadratic  $f_{ij}$  is an *epistatic contribution to fitness*. The goal of the line of research pursued in this paper is to find ways to retrieve the  $f_{ij}$  from the distribution of genotypes in a population.

The Quasi-Linkage Equilibrium (QLE) theory is based on approximating the genome distribution  $P$  as a Gibbs-Boltzmann distribution of the Ising/Potts type:

$$\log P(\mathbf{g}, t) = \Phi(t) + \sum_i \phi_i(t) s_i + \sum_{i < j} J_{ij}(t) s_i s_j, \quad (4)$$

In above  $\Phi(t)$  is a normalization factor playing the same role as  $-\beta F(\beta)$  in statistical mechanics. By expressing the evolution equations for  $P(\mathbf{g}, t)$  in terms of the effective parameters  $\Phi(t)$ ,  $\phi_i(t)$  and  $J_{ij}(t)$ , it was shown in [9–11], that the distribution (4) is stable at high rate of recombination. The values of the parameters  $\Phi$ ,  $\phi_i$  and  $J_{ij}$  in stationary state are then related to the model parameters as discussed in detail in [7, 11]. In particular,  $J_{ij}$  is simply proportional to  $f_{ij}$  which can be turned around to the *KNS fitness inference formula*

$$f_{ij}^* = J_{ij}^* \cdot r c_{ij}. \quad (5)$$

The stars on both sides indicate that these are inferred quantities, the proportionality parameters  $r$  and  $c_{ij}$  are discussed below.

In this work we have followed a different approach motivated by the analogy to physical kinetics. We start from the evolution equations for the first and second moments of the distribution which we obtain from the Boltzmann-like equation. These coupled equations will also depend on third and fourth moments. Applying the technique of Gaussian closure we estimate these higher moments in terms of first moment and second-order correlation function, and so obtain a set of closed and coupled equations for the temporal evolution of these quantities, respectively  $\chi_i \equiv \langle s_i \rangle$  and  $\chi_{ij} \equiv \langle s_i s_j \rangle - \chi_i \chi_j$ . The Gaussian closure treats the distribution as it were of the form (4) for continuous variables. As a consequence  $J_{ij} = -(\chi^{-1})_{ij}$  which in the DCA context amounts to the naive mean-field inference formula [13]. We emphasize that the meaning here is different: we actually do not assume that the full distribution is of the form (4) (or any other), only that it is appropriate to do so (with continuous variables) for the purpose of estimating moments.

We then study perturbatively the stationary solutions of the closed equations for  $\chi_{ij}$  obtained from the Gaussian closure in a scenario in which both mutations and recombination are present. This analysis leads to the following fitness inference formula

$$f_{ij}^* = \chi_{ij} \cdot \frac{(4\mu + r c_{ij})}{(1 - \chi_i^2)(1 - \chi_j^2)} \quad (6)$$

The mathematical derivation of the above result is summarized in Appendix A. We note that the combination  $\chi_{ij}/((1-\chi_i^2)(1-\chi_j^2))$  has previously appeared in epistatic fitness inference as approximation to  $J_{ij}$  [7, 11]. It is interesting to see the same formula reappear starting from other assumptions, and with a different factor of proportionality. The parameters  $\mu$ ,  $r$  and  $c_{ij}$  have the same meaning as in [11] and stand for mutation rate (assumed uniform) recombination rate (assumed uniform) and the probability of off-springs inheriting the genetic information from different parents. For high-recombination organisms,  $c_{ij}$  depends on the crossover rate  $\rho$  and the genomic distance between loci  $i$  and  $j$  [8].

$$c_{ij} \approx \frac{1}{2} \left(1 - e^{-2\rho|i-j|}\right) \quad (7)$$

except when loci  $i$  and  $j$  are very closely spaced on the genome.

When comparing (5) and (6) in numerical testing we simulate an evolving population at the same parameter values, and then either use the genotype information to compute empirical correlations, or to infer Ising/Potts parameters by DCA. For simplicity we will in the following only present results obtained by DCA naive mean-field (nMF) inference; results are very similar for other common variants of DCA.

### III. SIMULATION STRATEGIES AND RESULTS

The basic idea is to simulate the states of a population with  $N$  individuals (genome sequences) evolving under mutation, selection and recombination and genetic drift. As in previous work we have used the FFPopSim package developed by Zanini and Neher for this purpose [19]. Simulation and parameter settings are given in Appendix B.

In a QLE phase the outcomes of such simulations are trajectories of means  $\chi_i(t)$  and correlations  $\chi_{ij}(t)$  which in principle can be computed from the configuration of the population  $\mathbf{g}^{(s)}(t)$  at generation  $t$ . After a suitable relaxation period we take the set  $\mathbf{g}^{(s)}(t)$  to be independent samples from a distribution (4) with unknown direct couplings  $J_{ij}$ . We will throughout use the DCA algorithm naive mean-field (nMF) [22] to infer parameters  $J_{ij}$  from data for original KNS, for descriptions, see Appendices C.

The principle of the numerical testing is to infer epistatic fitness parameters from the data by (5) and (6), and then compare to the underlying parameters  $f_{ij}$  used to generate the data. Here, the testing epistatic fitness is Sherrington-Kirkpatrick model [23] with different variations. The additive fitness  $f_i$  follows Gaussian distribution with zero means and the standard deviation  $\sigma(\{f_i\}) = 0.05$  in our simulations. We note that (5) is proposed to be hold for weak selection and high recombination, and has already been tested in [8]. Data availability is an issue. As in [8] we have used *all-time* versions of the algorithms, where samples  $\mathbf{g}^{(s)}(t)$  at different  $t$  are pooled. This is primarily to mitigate the

effect that in a real-world population the number of individuals  $N$  is very large, but in the simulations it is only moderately large. All DCA methods as well as empirical correlations can be more accurately estimated, the more the samples.

#### A. Mutation vs recombination rate

We start by taking a fixed fitness landscape (same  $f_{ij}$ ) and systematically vary mutation and recombination ( $\mu$  and  $r$ ). Each sub-figure in large Fig. 1 shows scatter plots for the KNS fitness inference formula (5) and the formula (6) based on Gaussian closure vs the model parameter  $f_{ij}$  used to generate the data. These model parameters were independent Gaussian random variables specified by their standard deviation  $\sigma(\{f_i\})$  and  $\sigma(\{f_{ij}\})$  as hyper-parameters. The parameters  $J_{ij}^*$  which enter (5) are inferred by naive mean-field (nMF).

The variations in Fig. 1 are such that each column has the same recombination rate in the order low-medium-high from left to right, and each row has the same mutation rate in the order low-medium-high from top to bottom. In the top row both inference formulae work well, particularly for high recombination rate at the top right. In the middle and bottom rows the KNS formula does not work while the formula based on Gaussian closure still performs well, and in particular does not have systematic errors.

For comparison in more extensive parameter ranges we have quantified inference performance by normalized root of mean square error

$$\epsilon = \sqrt{\frac{\sum_{ij} (f_{ij}^* - f_{ij})^2}{\sum_{ij} f_{ij}^2}} \quad (8)$$

We note that this reduces all the information in the scatter plots in Fig. 1 to one single number. Although we have not observed such behaviour, it is conceivable that inference could be very accurate for most pairs  $(i, j)$  such that  $\epsilon$  is small, but still have large errors for some few pairs. An overall value  $\epsilon$  much less than one hence does not guarantee that fitness inference is accurate for all pairs. On the other hand, a large mean square error could correspond to either systematic or random errors in the scatter plots. behaviours which we have both observed.

With this proviso we point to phase diagrams of  $\epsilon$  shown in Fig. 2, for respectively KNS formula with nMF and the formula from Gaussian closure. Number of generations in simulations is set as  $T = 10,000$  and kept as a constant for all combinations of parameters. As in the scatter plots we observe large differences as to two epistatic fitness inference formulae. In short, for linear structure of genomes, the KNS formula (5) works only for low mutation rate and high recombination rate (Fig. 1c). The new formula (6) from Gaussian closure instead works for a much larger region with weak fitness. The standard deviation of epistatic fitness  $\sigma(\{f_{ij}\}) = 0.004$  in Fig. 2. We comment on the reasons for this effect in Section IV. For stronger mutation rate and larger re-

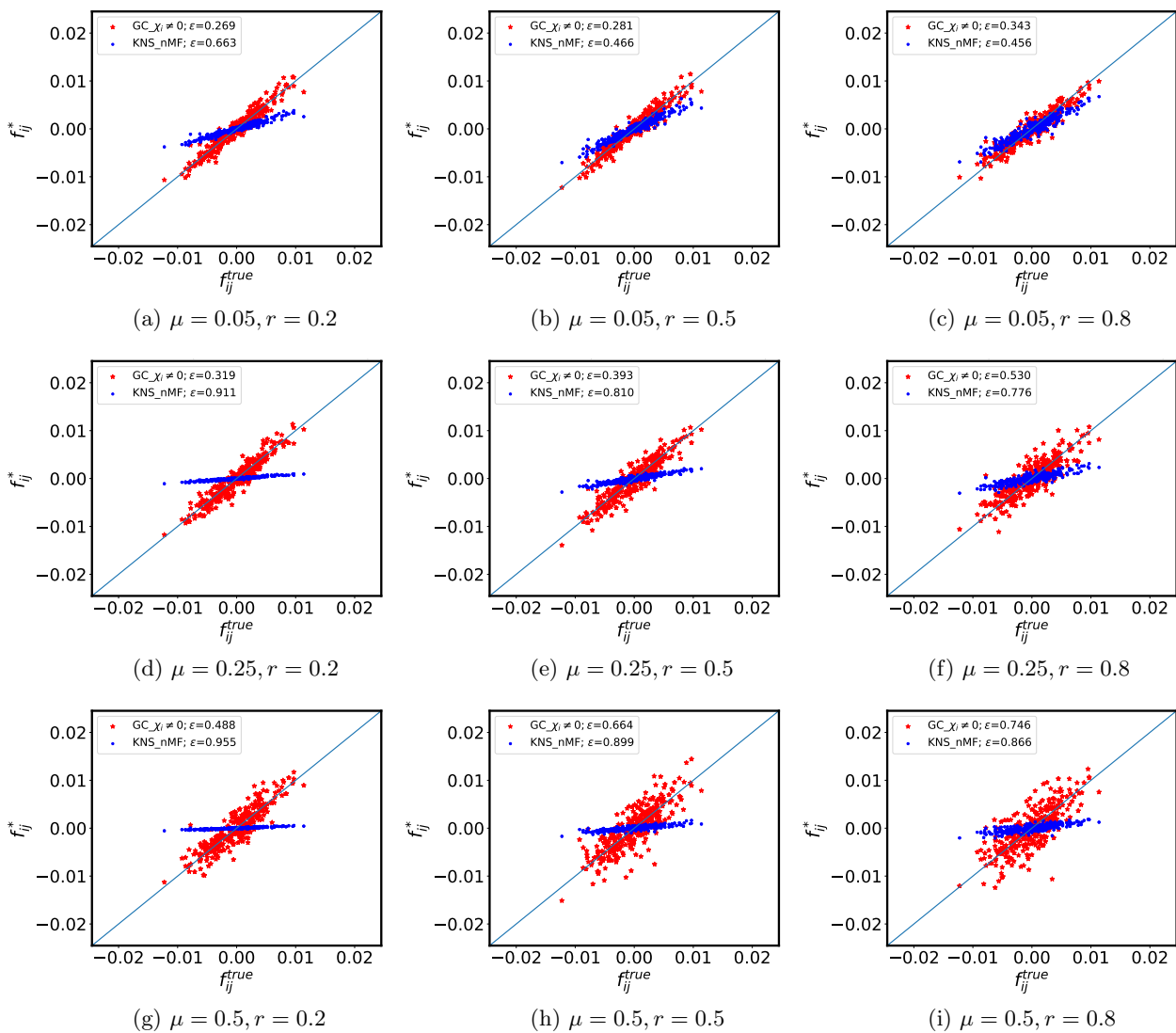


FIG. 1. Scatter plots for testing and recovered  $f_{ij}$ s with mutation rate  $\mu$  and recombination rate  $r$ .  $r$  increases from left to right columns (0.2, 0.5 and 0.8 respectively) while  $\mu$  enlarge from top to bottom (0.05, 0.25 and 0.5 respectively). The red stars for the Gaussian closed KNS  $f_{ij}^* = \chi_{ij} \cdot (4\mu + rc_{ij}) / ((1 - \chi_j^2)(1 - \chi_i^2))$ ; blue dots for original KNS  $f_{ij}^* = rc_{ij} \cdot J_{ij}^{*,nMF}$ . Other parameters:  $\sigma(\{f_i\}) = 0.05$ ,  $\sigma(\{f_{ij}\}) = 0.004$ , cross-over rate  $\rho = 0.5$ , number of loci  $L = 25$ , carrying capacity  $N = 200$ , number of generations  $T = 10,000$ . Inference by Gaussian closed KNS works in much wider parameter range than original KNS. One realization of the fitness terms  $f_{ij}$  and  $f_i$  for each parameter value.

combination rate (data not shown) the root mean square error ( $\epsilon$ ) of inference based on the Gaussian closure formula increases, *i.e.* in that range this formula does not work either. Specifically, the KNS formula (5) has severe systematic error while the formula (6) with Gaussian closure performs worse with heavier noise.

## B. Fitness variations vs recombination rate

We continue by varying recombination  $r$  and the dispersion in the fitness landscape ( $f_{ij}$  drawn from Gaussian distributions with different hyper-parameters  $\sigma(\{f_{ij}\})$ ). Each sub-figure in Fig. 3 shows scatter plots for the two epistatic fitness inference formulae for the model parameter  $\sigma(\{f_{ij}\})$  vs recombination rate  $r$ . The order in the Fig. 3 is increasing recombination rate  $r$  in columns from

left to right, and increasing  $\sigma(\{f_{ij}\})$  in rows from top to bottom. Here, the mutation rate  $\mu = 0.2$  and the other parameters are the same with those tested in Fig. 1.

Overall, the KNS formula (5) does not work for any of the parameter values shown in Fig. 3 with mutation rate  $\mu = 0.2$ . This either because of systematic errors as in top row (low fitness dispersion) and left column (low recombination), or due to large random scatter, as in bottom right corner Fig. 3h and Fig. 3i. The Gaussian closure formula (6) in contrast works well for (low recombination or low fitness dispersion, or both).

As above we have quantified inference performance in larger parameter ranges by the root of mean square error  $\epsilon$ . The phase diagrams in Fig. 4 show again that the Gaussian closure formula works except when  $r$  and  $\sigma(\{f_{ij}\})$  are both large, while the KNS formula does not work in any range with mutation rate  $\mu = 0.2$ .

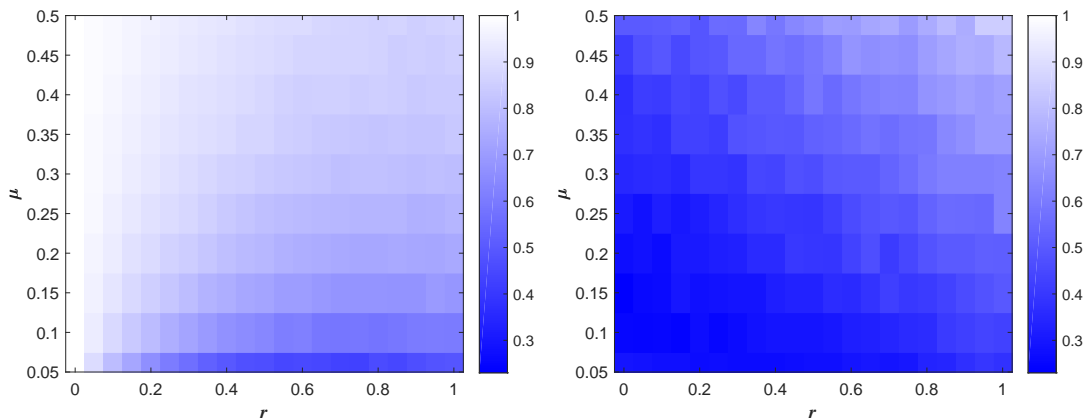


FIG. 2. Phase diagram for mutation rate  $\mu$  versus recombination rate  $r$ . The color is encoded by the reconstruction error  $\epsilon$  given in eq. (8). Left: KNS theory  $f_{ij} = J_{ij}^{*,nMF} \cdot rc_{ij}$ . Right: Gaussian closed KNS theory  $f_{ij} = \chi_{ij} \cdot (4\mu + rc_{ij}) / ((1 - \chi_i^2)(1 - \chi_j^2))$ . Parameters:  $\sigma(\{f_i\}) = 0.05$ ,  $\sigma(\{f_{ij}\}) = 0.004$ , cross-over rate  $\rho = 0.5$ , number of loci  $L = 25$ , carrying capacity  $N = 200$ , generations  $T = 10,000$ . One realization of the fitness terms  $f_{ij}$  and  $f_i$  for each parameter value.

#### IV. DISCUSSION

In this paper we have pursued the investigations started by Kimura in 1965 [9] on how epistatic contributions to fitness is reflected in the distribution over genotypes in a population. Our perspective is that of fitness inference: we assume that the distribution is observable from many whole-genome sequences of an organism and ask what we can learn about synergistic effects on fitness from concurrent allele variations at different loci, *i.e.* about epistasis. Our benchmark has been the generalization of the Kimura theory by Neher and Shraiman to a phase of genome-scale Quasi-Linkage Equilibrium (QLE) [7, 10, 11]. In recent work we showed in numerical testing that a central formula describing the QLE phase allows to retrieve epistatic contributions to fitness in the limit of high recombination [8].

Here we have followed a different path motivated by the analogy of physical kinetics and approximations of the Boltzmann equation [17, 18]. We have considered the evolution equations for single-locus and two-loci frequencies in a population evolving under selection, mutation, genetic drift and recombination, in the same set-up as [11], and then closed those equations by setting higher-order cumulants to zero (Gaussian closure). We hence do not make any explicit assumptions on the functional form of the distribution over genotypes in a population, only that it is possible to treat it as a Gaussian for the purpose of evaluating higher moments.

The phase diagrams in Fig. 2 and Fig. 4 in Section III show that the inference formula based on Gaussian closure dramatically outperforms the formula derived from the QLE phase, with the exception of a region at strong fitness and high recombination rate.

Inference formula (5) is obtained by perturbation in the inverse of recombination rate *i.e.* Eq. (23) and Appendix B in [11]. In a finite population this derivation requires that mutations are so much weaker compared to recombination that they can be neglected for quantitative properties in QLE, while still being non-zero. The latter restriction is necessary as otherwise the fittest

genotype will eventually take over the population, and the QLE phase will only be a long-lived transient [7, 8]. One consequence of a low mutation rate is that any imbalance in total epistatic fitness will lead to almost fixed alleles. In the QLE phase where Eq. (5) can be used quantitatively, the first order moments  $\chi_i$  are therefore typically different than zero. Inference formula (6) is on the other hand obtained in Appendix A by expanding the equations of Gaussian closure under conditions appropriate for high mutation rate, and  $\chi_i$  are not necessarily to be zero neither. A further assumption to arrive at (6) is that epistatic fitness variations are not too strong, qualitatively  $L\sigma(\{f_{ij}\}) < 1$ . Moreover, the additive fitness should be sufficiently weak as well to make sure the population is strictly mono-clonal which is one of the assumptions of the Gaussian closure [17, 18]. Data shown in bottom row of Fig. 3 (sub-figures (g), (h) and (i)) have  $L\sigma(\{f_{ij}\}) \approx 1$ .

The conclusions of this discussion are twofold. The first is that the new fitness inference method presented in this paper, while working in a much larger domain than the one based on the Kimura-Neher-Shraiman theory, cannot be the final answer. Combining reasoning and methods it should be possible to find further improvement in a unified treatment. We hope to return to this question in a future contribution. The second is that only a part of the properties of the QLE state are required for effective fitness inference. In fact, the main assumption in this work is a Boltzmann *Stosszahlansatz* for the two-genome distributions, and a standard Gaussian closure of the moments. Explicit assumptions on the underlying probability distributions are not needed. In particular, it is an open question whether fitness inference requires that the distribution over genotypes really has to be of form (4).

#### V. ACKNOWLEDGEMENTS

We are grateful to Guilhem Semerjian for valuable input and suggestions. The work of HLZ was spon-

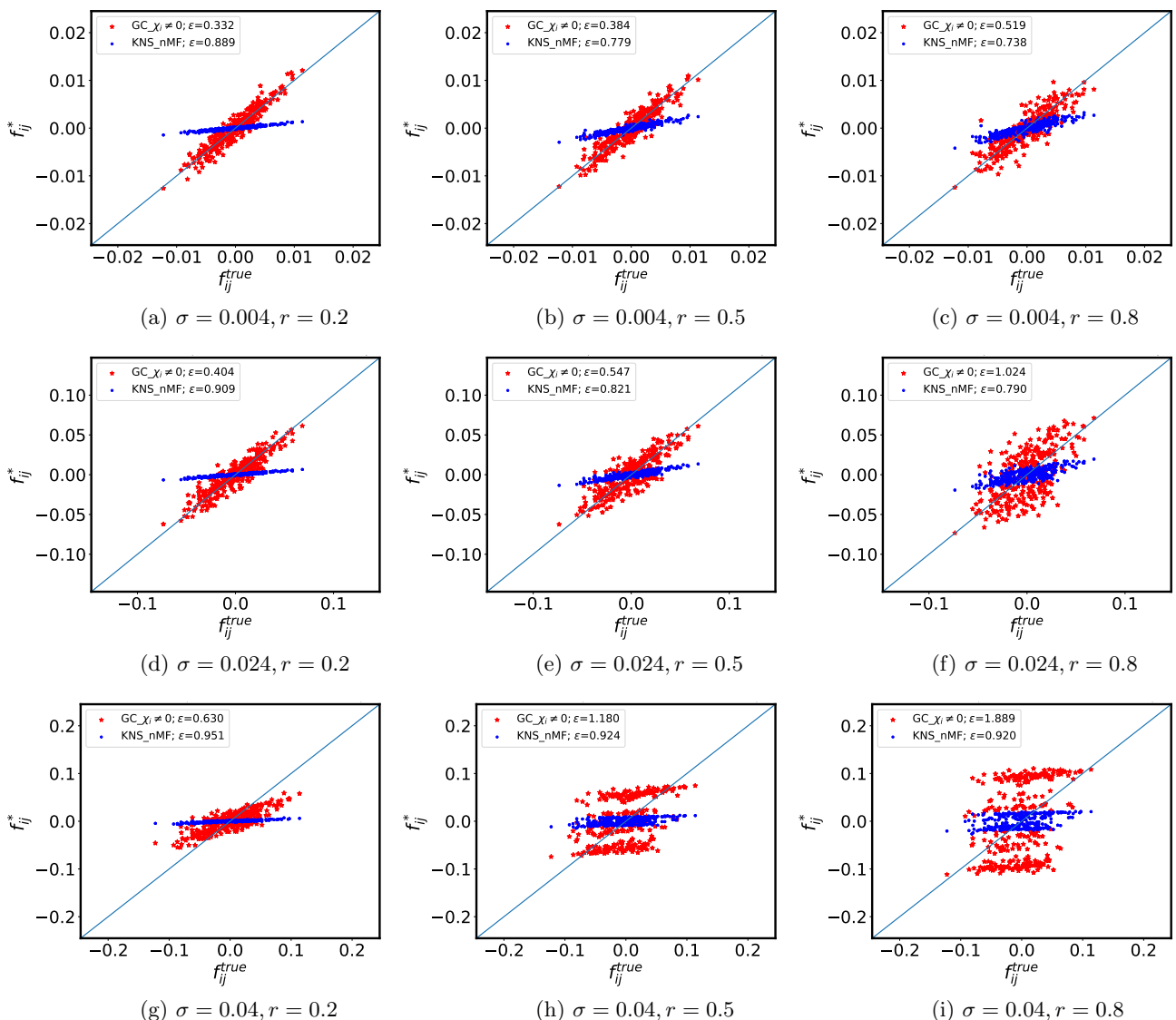


FIG. 3. Scatter plots for testing and reconstructed  $f_{ij}$ s. The standard deviation  $\sigma(\{f_{ij}\}^{true})$  increases from top to bottom rows (0.004, 0.024 and 0.04 respectively) and recombination rate  $r$  enlarges in columns from left to right (0.2, 0.5 and 0.8 respectively). Red stars for  $f_{ij}^* = \chi_{ij} \cdot (4\mu + rc_{ij}) / ((1 - \chi_i^2)(1 - \chi_j^2))$  and blue dots for  $f_{ij}^* = J_{ij}^{*,nMF} \cdot rc_{ij}$ . The other parameter values: standard deviation  $\sigma(\{f_i\}) = 0.05$ , mutation rate  $\mu = 0.2$ , cross-over rate  $\rho = 0.5$ , number of loci  $L = 25$ , carrying capacity  $N = 200$ , generations  $T = 10,000$ . Both inference formulae do not work for large  $\sigma$  and high  $r$ . One realization of the fitness terms  $f_{ij}$  and  $f_i$  for each parameter value.

sored by National Natural Science Foundation of China (11705097), Natural Science Foundation of Jiangsu Province (BK20170895), Jiangsu Government Scholarship for Overseas Studies of 2018. The work of EM was supported by ICFP fellowship and École Normale Supérieure (Paris). The work of VD was supported by Extra-Erasmus Scholarship (University of Trieste) and Collegio Universitario ‘Luciano Fonda’. SC and RM acknowledge financial support from the Agence Nationale de la Recherche projects RBMPPro (ANR-17-CE30-0021) and Decrypted (ANR-19-CE30-0021). EA acknowledge the Science for Life Labs (Solna, Sweden) ‘‘Viral sequence evolution research program’’.

## Appendix A: Evolution under selection, mutations and recombination

In this Appendix we introduce the model defined in [11] for the evolution of the distribution of genomes  $P(\mathbf{g}, t)$  and describe the fitness inference procedure derived in [17, 18]. Throughout we assume an infinite population; genetic drift is therefore not considered.

Selection is the first fundamental ingredient and works as follows: each possible sequence  $\mathbf{g}$  grows inside the population with a certain growth-rate  $F(\mathbf{g})$ , called *fitness*, which can be described as a function of the specific sequence  $\mathbf{g}$ . In general, any function  $F$  of this type can be

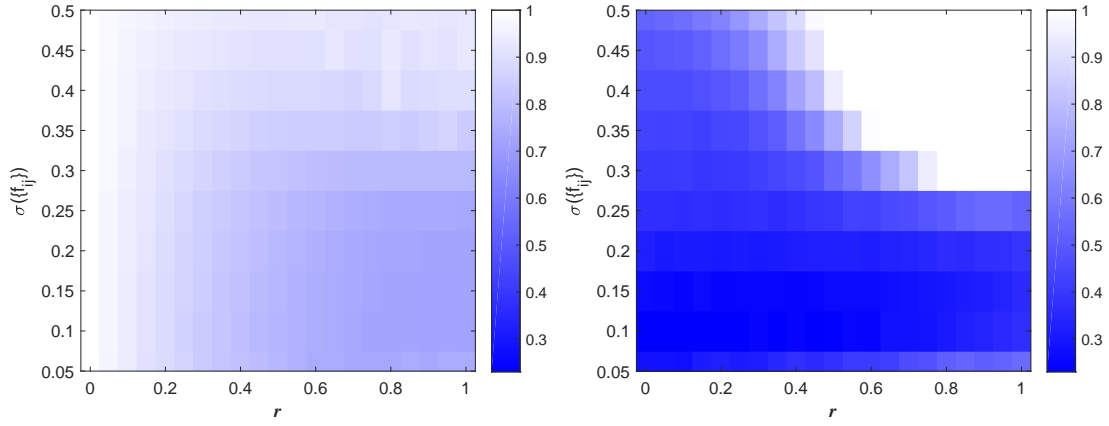


FIG. 4. Phase diagram for the standard deviation  $\sigma(\{f_{ij}\})$  versus recombination rate  $r$ . Left: KNS theory  $f_{ij}^* = J_{ij}^{nMF} \cdot rc_{ij}$ . Right: Gaussian closed KNS theory  $f_{ij}^* = \chi_{ij} \cdot (4\mu + rc_{ij}) / ((1 - \chi_i^2)(1 - \chi_j^2))$ . Parameters: mutation rate  $\mu = 0.2$ , cross-over rate  $\rho = 0.5$ , number of loci  $L = 25$ , carrying capacity  $N = 200$ , generations  $T = 10,000$ . One realization of the fitness terms  $f_{ij}$  and  $f_i$  for each parameter value.

decomposed in the following way

$$F(\mathbf{g}) = \bar{F} + \sum_i f_i s_i + \sum_{i < j} f_{ij} s_i s_j + \sum_{i < j < k} f_{ijk} s_i s_j s_k + \dots \quad (\text{A1})$$

Following the discussion in the main body of the paper we have neglected all interactions with order higher than two. We consider hence only  $f_i$  and  $f_{ij}$  referred to *additive fitness* and *epistatic fitness* respectively.

The second ingredient for the evolution of the system are mutations. We assume that in each small time interval  $\Delta t \ll 1$  a fraction  $\mu\Delta t$  of all the alleles inside the population ( $L$  for each individual) mutate by a single spin-flip;  $\mu$  is therefore named mutation rate. We describe the process of a spin flip by introducing an operator  $M_i$  acting on a sequence by changing the sign of the  $i$ -th spin. To understand how the frequency of a certain sequence  $\mathbf{g}$  changes in the interval  $\Delta t$ , we should count how many individuals have mutated into the sequence  $\mathbf{g}$  and how many sequences have instead mutated from away this state.

The last element to consider is recombination between different sequences. At each small time interval  $\Delta t$  a fraction  $r\Delta t$  of the individuals (where  $r$  is the recombination rate) encounters random pairing and out-crossing, giving rise to new genomes. The evolution of the distribution  $P$  in the interval  $\Delta t$  due to recombination is given by

$$P(\mathbf{g}, t + \Delta t) = (1 - r\Delta t)P(\mathbf{g}, t) + r\Delta t \sum_{\{s'_i\}\{\xi_i\}} C(\{\xi\}) P(\mathbf{g}^{(m)}, t) P(\mathbf{g}^{(f)}, t). \quad (\text{A2})$$

The first term counts for those individuals that did not recombine during the time interval  $\Delta t$ . When two individuals recombine, a new genotype is formed by inheriting some loci from the mother with genotype  $\mathbf{g}^{(m)}$  and the complement from the father with genotype  $\mathbf{g}^{(f)}$ . The parts of the genomes of the mother and the father not inherited by the child (and hence discarded) is denoted  $\mathbf{g}'$ . The cross-over can be described by a vector  $\{\xi_i\}$ , with  $\xi_i \in \{0, 1\}$ . If  $\xi_i = 1$ , the  $i$ -th locus is inher-

ited from the mother, otherwise by the father. Turning around the relation we have  $s_i^{(m)} = s_i \xi_i + s'_i (1 - \xi_i)$  and  $s_i^{(f)} = s'_i \xi_i + s_i (1 - \xi_i)$  where  $s_i$  is the allele of the child at locus  $i$ , and  $s'_i$  is the discarded allele. The probability of each realization of  $\{\xi_i\}$  is given by  $C(\{\xi\})$ . Subsequently we need to sum over all the possible genomes which are not passed on the offspring ( $\mathbf{g}'$ ) as well as all the possible crossover patterns  $\{\xi\}$  [7, 11].

Merging together all the ingredients, we obtain the following non-linear differential equation for the time derivative of  $P$ :

$$\begin{aligned} \dot{P}(\mathbf{g}, t) &= \\ &= \frac{d}{dt}|_{\text{fitness}} P(\mathbf{g}, t) + \frac{d}{dt}|_{\text{mut}} P(\mathbf{g}, t) + \frac{d}{dt}|_{\text{rec}} P(\mathbf{g}, t) = \\ &= [F(s) - \langle F \rangle] P(\mathbf{g}, t) + \mu \sum_{i=0}^{L-1} [P(M_i \mathbf{g}, t) - P(\mathbf{g}, t)] + \\ &+ r \sum_{\{s'_i\}\{\xi_i\}} C(\{\xi\}) [P(\mathbf{g}^{(m)}, t) P(\mathbf{g}^{(f)}, t) - P(\mathbf{g}, t) P(\mathbf{g}', t)]. \end{aligned} \quad (\text{A3})$$

Going forward, we want to parameterize the distribution  $P(\mathbf{g}, t)$  by its cumulants. In particular, we define the cumulants of first and second order as  $\chi_i \equiv \langle s_i \rangle$  and  $\chi_{ij} \equiv \langle s_i s_j \rangle - \chi_i \chi_j$ . Note that in this way  $\chi_{ii} = 1 - \chi_i^2$ . Using Eq. (A3), we can write the time evolution for these cumulants as follows:

$$\dot{\chi}_i = \langle s_i [F(\mathbf{g}) - \langle F \rangle] \rangle - 2\mu \chi_i \quad (\text{A4})$$

$$\begin{aligned} \dot{\chi}_{ij} &= \langle (s_i - \chi_i)(s_j - \chi_j) [F(\mathbf{g}) - \langle F \rangle] \rangle + \\ &- (4\mu + rc_{ij}) \chi_{ij}, \end{aligned} \quad (\text{A5})$$

with  $i \neq j$  in the second line. Here we have defined  $c_{ij} \equiv \sum_{\{\xi\}} C(\{\xi\}) [\xi_i (1 - \xi_j) + (1 - \xi_i) \xi_j]$  a quantity which represents the probability that loci  $i$  and  $j$  arrive from different parents.

In general, Eq. (A4) and (A5) are not a closed set of equations since they would also depend on higher order cumulants  $\chi_{ijk}$ ,  $\chi_{ijkl}$ , etc. The Gaussian closure which

we introduced recently [18] aims to overcome this problem by neglecting those higher order cumulants (connected correlation functions) under the assumption that at high recombination and/or mutations rate their influence on the global dynamics is weak. For a Gaussian distribution, all cumulants of order higher than two vanish. With this approximation, (A4) and (A5) define a closed set of  $L(L+1)/2$  dynamical equations only depending on  $\chi_i$  and  $\chi_{ij}$ .

$$\dot{\chi}_i = \sum_j \chi_{ij} \left( f_j + \sum_k f_{jk} \chi_k - 2f_{ij} \chi_i \right) - 2\mu \chi_i \quad (\text{A6})$$

$$\begin{aligned} \dot{\chi}_{ij} = & -2\chi_{ij} \sum_k \left[ f_{ik} (\chi_{ik} + \chi_i \chi_k) + f_{jk} (\chi_{jk} + \chi_j \chi_k) \right] + \\ & + 2f_{ij} \chi_{ij} (\chi_{ij} + 2\chi_i \chi_j) + \sum_{k,l} f_{kl} \chi_{ik} \chi_{jl} + \\ & - (4\mu + rc_{ij}) \chi_{ij} - 2\chi_{ij} (f_i \chi_i + f_j \chi_j) \end{aligned} \quad (\text{A7})$$

In principle, Eq. (A6)-(A7) could be simultaneously solved in order to determine the stationary state, which is of our interest, and this in turn would allow to determine the  $L(L+1)/2$  quantities  $\{f_i\}, \{f_{ij}\}$  as a function of the  $\{\chi_i\}, \{\chi_{ij}\}$ . Unfortunately, considering the size of the system, this is analytically not feasible.

Nevertheless, Eq. (A7) suggests another route to infer  $f_{ij}$  according to the following argument: when studying the stationary state, we can assume self-consistently that all the off-diagonal  $\chi_{ij}$  are small, so that we can expand  $\chi_{ij}$ , with  $i \neq j$ , as a power series of  $1/(4\mu + rc_{ij})$ :

$$\chi_{ij} = \frac{\chi_{ij}^{(1)}}{4\mu + rc_{ij}} + \mathcal{O}((4\mu + rc_{ij})^{-2}). \quad (\text{A8})$$

Inserting this in Eq.(A7), we obtain

$$\chi_{ij}^{(1)} = f_{ij} (1 - \chi_i^2) (1 - \chi_j^2). \quad (\text{A9})$$

We therefore conclude that, to the first order,

$$\chi_{ij} = \frac{f_{ij}}{4\mu + rc_{ij}} (1 - \chi_i^2) (1 - \chi_j^2). \quad (\text{A10})$$

Turning around this into an inference formula for fitness we arrive at (6) in the main body of the paper.

As a final remark, it is straightforward to compute from Eq. (A7) higher order terms in the expansion for  $\chi_{ij}$ . For instance, in the case where  $f_i = 0$  for all  $i$  we find

$$\chi_{ij} = \frac{f_{ij}}{4\mu + rc_{ij}} + \frac{2}{(4\mu + rc_{ij})^2} \sum_k f_{ik} f_{jk} + \dots \quad (\text{A11})$$

We observe that the second-order correction is negligible if  $L \times \sigma(\{f_{ij}\}) \ll 1$  therefore in this regime we may expect the first-order to be accurate.

## Appendix B: FFPopSim settings

The FFPopSim package, written by Fabio Zanini and Richard Neher simulates a population evolving due to mutation, selection and recombination [19].

In this paper we have used FFPopSim in a similar manner as in [8] and we will here only list the settings. Parameters which are the same in all simulations reported in this paper are listed in Tab. I. Parameters that have been varied (not all variations reported in the paper) are listed in Tab. II.

It is important to notice that the out-crossing rate  $r$  in FFPopSim *a priori* differs from our recombination rate,  $r$ , appearing in Eq. (6). In the simulation package, dynamics is discrete in time (with time step of one generation) and  $r$  is a probability taking value between 0 and 1. In our theory,  $r$  is a rate, which can take any positive value. In the examples given in [19], e.g. Fig 2 in the main text and Fig 2 in Supplementary Information the out-crossing probability does not exceed  $10^{-2}$ . For such low values  $r$  coincides with a rate (since the time step is equal to unity), which justifies its denomination. We use this correspondence between the out-crossing rate  $r$  in FFPopSim and our recombination rate  $r$ , valid for small values, to produce the scatter plots in Figs. 1 and 3.

Notice that this correspondence breaks down for large recombination rates. Indeed, even for out-crossing rate  $r = 1$  in the simulation package, mutations and fitness effects can still be quite large, depending on the values of the  $f_{ij}$ 's and of  $\mu$ , and QLE is not recovered. In the theory, however, all fitness and mutation effects become relatively weak, of the order of  $1/r$ .

TABLE I. Main default parameters of FFPopSim used in the simulations.

number of loci (L)	25
number of traits	1
circular	False
carrying capacity (N)	200
generation	10,000
recombination model	CROSSOVERS
crossover rate ( $\rho$ )	0.5
fitness additive(coefficients)	Gaussian random
	number with standard
	deviation $\sigma(\{f_i\}) = 0.05$

TABLE II. Variable parameters of FFPopSim used in the simulation.

initial genotypes	binary random numbers
out-crossing rate ( $r$ )	[0., 1.0]
mutation rate ( $\mu$ )	[0.05, 0.5]
epistatic fitness	Gaussian random
	number with standard deviation
	$\sigma(\{f_{ij}\}) \in [0.004, 0.04]$

### Appendix C: Naive mean-field use (nMF)

Naive mean-field is based on minimizing the reverse Kullback-Leibler distance between an empirical probability distribution and a trial distribution in the family of independent (factorized) distributions. This leads to the *inference formula*  $J_{ij}^{*,nMF} = (\chi^{-1})_{ij}$ . If the correlation  $\chi_{ij}$  is computed as an average over the population at a single time we call it *single-time-nMF*. If on the other hand  $\chi_{ij}$  is computed by additionally averaging over time we call it *all-time-nMF*.

The pseudo-code for nMF inference taking  $\chi_{ij}$  as input is presented in Algorithm 1.

---

**Algorithm 1:** Epistatic fitness inference by KNS formula (5) with  $J_{ij}^*$  reconstructed by nMF

---

procedure:  $f_{ij}^{nMF}$

---

**Input:** mean correlations:  $\langle \chi_{ij} \rangle$

**Output:** inferred epistatic fitness:  $f_{ij}^{nMF}$

```

1: import scipy
2: from scipy import linalg
3:  $J_{ij}^{nMF} = - \text{linalg.inv}(\langle \chi_{ij} \rangle)$ 
4:  $f_{ij}^{nMF} = J_{ij}^{nMF} * rc_{ij}$ 

```

---

- [1] J. A. G. de Visser and J. Krug, Nature Reviews Genetics **15**, 480 (2014).
- [2] J. M. Smith, *Evolution and the Theory of Games* (Cambridge University Press, 1982).
- [3] E. Chastain, A. Livnat, C. Papadimitriou, and U. Vazirani, Proceedings of the National Academy of Sciences **111**, 10620 (2014), <https://www.pnas.org/content/111/29/10620.full.pdf>.
- [4] Y. Shu and J. McCauley, Eurosurveillance **22** (2017), <https://www.gisaid.org/>.
- [5] T. Bedford, R. Neher, J. Hadfield, E. Hodcroft, T. Sibley, J. Huddleston, J. Lee, K. Fay, S. Bell, C. Megill, B. Potter, P. Sagulenko, C. Callender, M. Ilcisin, L. Moncla, A. Black, A. Brito, and N. Grubaugh, "Nextstrain," <https://nextstrain.org/>, Trevor Bedford and Richard Neher (2015-2020).
- [6] J. Hadfield, C. Megill, S. M. Bell, J. Huddleston, B. Potter, C. Callender, P. Sagulenko, T. Bedford, and R. A. Neher, Bioinformatics **34**, 4121 (2018), <https://academic.oup.com/bioinformatics/article-pdf/34/23/4121/26676762/bty407.pdf>.
- [7] C.-Y. Gao, F. Cecconi, A. Vulpiani, H.-J. Zhou, and E. Aurell, Phys. Biol. **16**, 026002 (2019).
- [8] H.-L. Zeng and E. Aurell, Phys. Rev. E **101**, 052409 (2020).
- [9] M. Kimura, Genetics **52**, 875 (1965).
- [10] R. A. Neher and B. I. Shraiman, Proc. Natl. Acad. Sci. **106**, 6866 (2009).
- [11] R. A. Neher and B. I. Shraiman, Rev. Mod. Phys. **83**, 1283 (2011).
- [12] Y. Roudi, E. Aurell, and J. A. Hertz, Front. Comput. Neurosci. **3**, 1 (2009).
- [13] H. C. Nguyen, R. Zecchina, and J. Berg, Adv. Phys. **66**, 197 (2017).
- [14] F. Morcos, A. Pagnani, B. Lunt, A. Bertolino, D. S. Marks, C. Sander, R. Zecchina, J. N. Onuchic, T. Hwa, and M. Weigt, Proc. Natl. Acad. Sci. **108**, E1293 (2011).
- [15] R. R. Stein, D. S. Marks, and C. Sander, PLoS Comput. Biol. **11**, e1004182 (2015).
- [16] S. Cocco, C. Feinauer, M. Figliuzzi, R. Monasson, and M. Weigt, Rep. Prog. Phys. **81**, 032601 (2018).
- [17] E. Mauri, "Population genetics and epistasis: a gaussian approximation for allele dynamics," École Normale Supérieure, Master ENS ICFP internship report (2019).
- [18] E. Mauri, S. Cocco, and R. Monasson, "Gaussian closure scheme for evolving genomes: theory and applications to short-range fitness model," in preparation (2020).
- [19] F. Zanini and R. A. Neher, Bioinformatics **28**, 3332 (2012).
- [20] R. Fisher, *The Genetical Theory of Natural Selection* (Clarendon, 1930).
- [21] R. A. Blythe and A. J. McKane, J. Stat. Mech.: Theory Exp. **2007**, P07018 (2007).
- [22] H. J. Kappen and F. B. Rodríguez, Neural Comput. **10**, 1137 (1998).
- [23] D. Sherrington and S. Kirkpatrick, Phys. Rev. Lett. **35**, 1792 (1975).